Cellular Signalling 26 (2014) 19–31

Contents lists available at ScienceDirect

Cellular Signalling

journal homepage: www.elsevier.com/locate/cellsig

# Inhibition of late endosomal maturation restores Wnt secretion in *Caenorhabditis elegans vps-29* retromer mutants

Magdalena J. Lorenowicz [a,1], Marie Macurkova [a,b], Martin Harterink [a], Teije C. Middelkoop [a], Reinoud de Groot [a], Marco C. Betist [a], Hendrik C. Korswagen [a,*]

[a] Hubrecht Institute, Royal Netherlands Academy of Arts and Sciences and University Medical Center Utrecht, Uppsalalaan 8, 3584 CT Utrecht, The Netherlands
[b] Department of Cell Biology, Faculty of Science, Charles University Prague, Vinicna 7, 128 00 Prague 2, Czech Republic

ARTICLE INFO

*Article history:*
Received 22 August 2013
Received in revised form 5 September 2013
Accepted 13 September 2013
Available online 20 September 2013

*Keywords:*
Retromer
Wnt
Wntless
Membrane trafficking
*Caenorhabditis elegans*

ABSTRACT

Secretion of Wnt proteins is mediated by the Wnt sorting receptor Wls, which transports Wnt from the Golgi to the cell surface for release. To maintain efficient Wnt secretion, Wls is recycled back to the *trans*-Golgi network (TGN) through a retromer dependent endosome to TGN retrieval pathway. It has recently been shown that this is mediated by an alternative retromer pathway in which the sorting nexin SNX3 interacts with the cargo-selective subcomplex of the retromer to sort Wls into a retrieval pathway that is morphologically distinct from the classical SNX-BAR dependent retromer pathway. Here, we investigated how sorting of Wls between the two different retromer pathways is specified. We found that when the function of the cargo-selective subcomplex of the retromer is partially disrupted, Wnt secretion can be restored by interfering with the maturation of late endosomes to lysosomes. This leads to an accumulation of Wls in late endosomes and facilitates the retrieval of Wls through a SNX-BAR dependent retromer pathway. Our results are consistent with a model in which spatial separation of the SNX3 and SNX-BAR retromer complexes along the endosomal maturation pathway as well as cargo-specific mechanisms contribute to the selective retrieval of Wls through the SNX3 retromer pathway.



## 1. Introduction

During the development of complex multi-cellular organisms, intercellular communication is critical for the growth and organization of cells into tissues and organs. One class of signaling molecules that play a central role during development and adult tissue homeostasis are the Wnt proteins [1]. Wnts are members of an evolutionarily conserved family of secreted, lipid modified glycoproteins that can function as short range signaling molecules, but also as morphogens that form concentration gradients to provide positional information to cells in developing tissues [2]. Although detailed insight has been obtained in the signaling pathways that are triggered by Wnt proteins, the mechanism of Wnt production and secretion is still poorly understood.

The discovery of the Wnt binding protein Wntless (Wls, also known as Evi or Sprinter in *Drosophila* and MIG-14 in *Caenorhabditis elegans*) [3–5] has provided important insight into the Wnt secretion mechanism. In *wls* mutant clones in the *Drosophila* wing imaginal disc, the Wnt protein Wg fails to be secreted and accumulates in producing cells, consistent with an essential function of Wls in the Wnt secretion pathway. Wls is a multi-pass transmembrane protein that localizes to the Golgi network, endosomes and the plasma membrane. Furthermore, Wls binds Wnt in co-immunoprecipitation experiments, supporting the notion that it functions as a sorting receptor that transports Wnt from the Golgi to the cell surface for release. At the plasma membrane, Wls is internalized through AP-2 adaptin and clathrin dependent endocytosis and is recycled back to the Golgi, a process that is critical for efficient Wnt secretion [6–10].

A key step in the retrieval of Wls is mediated by the retromer complex [11,12]. The retromer is a multi-protein coat complex that is recruited to endosomes to transport transmembrane proteins such as the yeast acid hydrolase receptor Vps10p and the mammalian cation-independent mannose-6-phosphate receptor (CI-MPR) to the TGN [13–15]. The retromer is also required for endosome-to-TGN transport of Wls [6–10]. In the absence of retromer function, Wls fails to be retrieved from the endosomal system and is degraded in lysosomes. As a result, Wls protein levels and Wnt secretion are reduced, leading to various phenotypes associated with loss of Wnt signaling [11,12].

The retromer consists of a stable trimer of the subunits Vps35, Vps26 and Vps29 and a membrane bound heterodimer of the SNX-BAR sorting nexins SNX1/SNX2 and SNX5/SNX6 [16–18]. The Vps29–26–35 trimer and the SNX-BAR heterodimer have distinct functions in cargo recognition and transport carrier formation. The Vps26–29–35 trimer directly binds to a loosely defined consensus sequence in the cytoplasmic tail of the cargo protein [19,20]. At the same time, the Vps26–29–35 trimer also interacts with the SNX-BAR heterodimer, which is recruited to the

* Corresponding author. Tel.: +31 30 2121981; fax: +31 30 2516464.
*E-mail address:* r.korswagen@hubrecht.eu (H.C. Korswagen).
[1] Present address: Department of Cell Biology, University Medical Center, Heidelberglaan 100, 3584CX Utrecht, The Netherlands.

0898-6568/$ – see front matter © 2013 Elsevier Inc. All rights reserved.
http://dx.doi.org/10.1016/j.cellsig.2013.09.013

endosomal membrane through phosphatidylinositol-3-phosphate (PI3P) binding Phox-homology (PX) domains. The interaction with the cargo-selective Vps26–29–35 sub-complex is thought to increase the effective concentration of SNX-BAR heterodimers, initiating a membrane remodeling process in which the membrane curvature sensing BAR domains of the SNX-BAR heterodimers drive the generation of tubules in which the cargo protein is segregated [18,21–24]. Scission of these retromer-decorated tubules produces specific transport carriers that traffic the cargo back to the TGN.

The process of retromer recruitment and cargo retrieval is closely linked to the endosomal maturation pathway. The maturation of early endosomes into late endosomes and the subsequent fusion of late endosomes with lysosomes are regulated by the sequential activity of the small GTPases Rab5 and Rab7 [25]. Recent evidence suggests that the Rab5 to Rab7 conversion mechanism also controls retromer recruitment, restricting the formation of retromer tubules to endosomes that are at the early-to-late transition point [24,26–29]. Rab7 has a direct role in this process by binding to a conserved region in the Vps35 subunit of the Vps26–29–35 sub-complex [30]. By recruiting the Vps26–29–35 trimer, Rab7 may coordinate the selection of cargo with SNX-BAR sorting nexin binding and tubule formation at early-to-late endosomes.

In contrast to retromer cargo proteins such as Vps10p, Sortilin and the CI-MPR [13–15], endosome-to-TGN retrieval of Wls is independent of the SNX-BAR sorting nexins SNX1 and SNX6 [31]. We have recently shown that Wls retrieval requires SNX3, an alternative sorting nexin that contains a PI3P binding PX domain for association with endosomal membranes, but lacks the membrane curvature sensing BAR domain that is present in the SNX-BAR sorting nexins. SNX3 directly interacts with the Vps26–29–35 trimer and sorts Wls into a retrieval pathway that is morphologically distinct from the SNX-BAR dependent retromer pathway, producing small transport vesicles instead of the tubular carriers formed by the SNX-BAR pathway. In the absence of SNX3, membrane association of Vps26 is reduced, indicating that SNX3 contributes to the recruitment of the cargo-selective Vps26–29–35 trimer to endosomal membranes.

In both the SNX3 and SNX-BAR retromer pathways, cargo binding is mediated by the Vps29–26–35 trimer. An important question is therefore how cargo is differentially sorted between the two pathways. In this study, we used a mutation in the *C. elegans* retromer subunit gene *vps-29* to partially disrupt retromer function. We found that Wnt secretion can be restored by inhibiting late endosomal maturation and that this rescue depends on retrieval of Wls through a SNX-BAR dependent retromer pathway. Our results are consistent with a model in which differences in endosomal localization as well as cargo-specific mechanisms contribute to the selective retrieval of Wls through the SNX3 retromer pathway.

## 2. Materials and methods

### 2.1. C. elegans strains and culturing

General methods for culture, manipulation and genetics of *C. elegans* were as described [32]. Strains were cultured at 20 °C. Strains, mutations and integrated arrays used in this study were Bristol N2: LGI, *snx-3(tm1595)* [31]; LGII, *muIs32[Pmec-7::gfp]* [33], *huSi2[Pmig-14::mig-14::gfp]* [34], *tbc-2(tm2241)* [35]; *vps-35(hu68)* [12]; LGIII, *vps-29(tm1320)* [12]; LGIV, *sand-1(ok1963)* [36]; *huIs60[Pegl-20::egl-20::protA]* [12]; LGV, *ccz-1(ok2182)* [36,37], *muIs35[Pmec-7::gfp]* [33]; LGX, *snx-1(tm847)* [12] and unassigned *huIs71[Pmig-14::mig-14::gfp]* [10].

### 2.2. C. elegans phenotypic analysis, RNA interference and expression constructs

To examine effects on QL.d migration, animals were grown at 20 °C on NGM agar plates seeded with control or gene specific dsRNA expressing bacteria as described [38,39]. The final position of the QL descendant QL.paa (PVM) was determined in L4 larvae or young adults using the *mec-7::gfp* transgenes *muIs32* or *muIs35* [33]. Migration was regarded as defective when the QL.d localized anterior to the vulva. For *snx-1(tm847)* and *snx-3(tm1595)*, the positions of QL.paa and QL.pap were scored by DIC microscopy in synchronized L1 larvae as described [12]. To construct *Pegl-20::mCherry::rab-7*, *rab-7* cDNA was fused with *mcherry* and cloned behind a 4.4 kb *egl-20* promoter fragment into vector pPD49.26. To generate *Pegl-20::mCherry::rab-7T23N*, a C at position 68 and an A at position 69 of the *rab-7* cDNA sequence were changed into an A and a T, respectively, using the QuikChange Site-Directed Mutagenesis kit (Stratagene). To construct *Pegl-20::sand-1::gfp*, *sand-1* cDNA was cloned in frame with *gfp* behind the *egl-20* promoter fragment in pPD95.81. To construct *Pegl-20::tbc-2*, *tbc-2* cDNA was cloned behind the *egl-20* promoter fragment in pPD49.26. To construct *Pmyo-3::mCherry::rab-5*, *rab-5* cDNA was cloned behind the *myo-3* promoter fragment and in frame with *mcherry* into pPD95.86. *Pmyo-2::tdTomato* was used as a co-injection marker for the generation of extra-chromosomal transgenes as described [40].

### 2.3. C. elegans fluorescent in situ hybridization (FISH), immunostaining and microscopy

*C. elegans* single molecule mRNA FISH and the design of the *mig-14* probe were performed as described [41]. For confocal microscopy, animals were immobilized in 30 mM sodium azide. Staining of EGL-20::Protein A was performed as described [12], but using a Cy5-coupled rabbit anti-goat antibody (Jackson Immunoresearch Laboratories). Images were collected on a Leica DM6000 wide field or Leica SPE confocal microscope. The intensity of the EGL-20::Protein A signal along the anteroposterior axis was quantified using a semi-automated MATLAB image processing tool. Assuming a single animal per image, we first manually found the animal's silhouette in the image. Next, by applying a regular skeletonization algorithm we found the animal's anteroposterior axis. The signal intensity was computed along this axis. For each point on the anteroposterior axis, we found the normal line, called here a slice (for a given point, a slice is perpendicular to the tangent line at this point). The signal intensity value $g(i)$ at point $i$ was taken as the maximum pixel intensity of pixels located in the corresponding slice. For statistical analysis, the exponential decay function curves were fitted to the series of EGL-20 signal intensity measurements along the anteroposterior axis. The exponential decay constants corresponding to the decay rate of the EGL-20 signal intensity curves were used to quantify statistical differences between the different experimental conditions. Levels of MIG-14::GFP were quantified using ImageJ software.

## 3. Results

### 3.1. Mutation of the cargo-selective retromer subunit gene vps-29 induces a partial block in EGL-20/Wnt signaling

Mutations that block the Golgi retrieval of the *C. elegans* Wls ortholog MIG-14 interfere with Wnt secretion and induce defects in several Wnt dependent processes [10]. One of the most prominent phenotypes is a defect in the migration of the left Q neuroblast descendants (QL.d) [12]. During the first stage of larval development, the QL.d migrate from the mid-body to well defined positions in the posterior (Fig. 1A). One of the principal regulators of this migration is the Wnt protein EGL-20, which activates a transcriptional program in the QL neuroblast (the expression of the Hox gene *mab-5*) that directs migration of the QL.d towards the posterior [42]. When EGL-20 signaling is reduced or absent, this program fails to be activated and as a consequence, the QL.d migrate in the opposite, anterior direction (here referred to as a QL.d migration defect). The final localization of the QL.d therefore provides a sensitive assay to measure EGL-20/Wnt signaling activity.

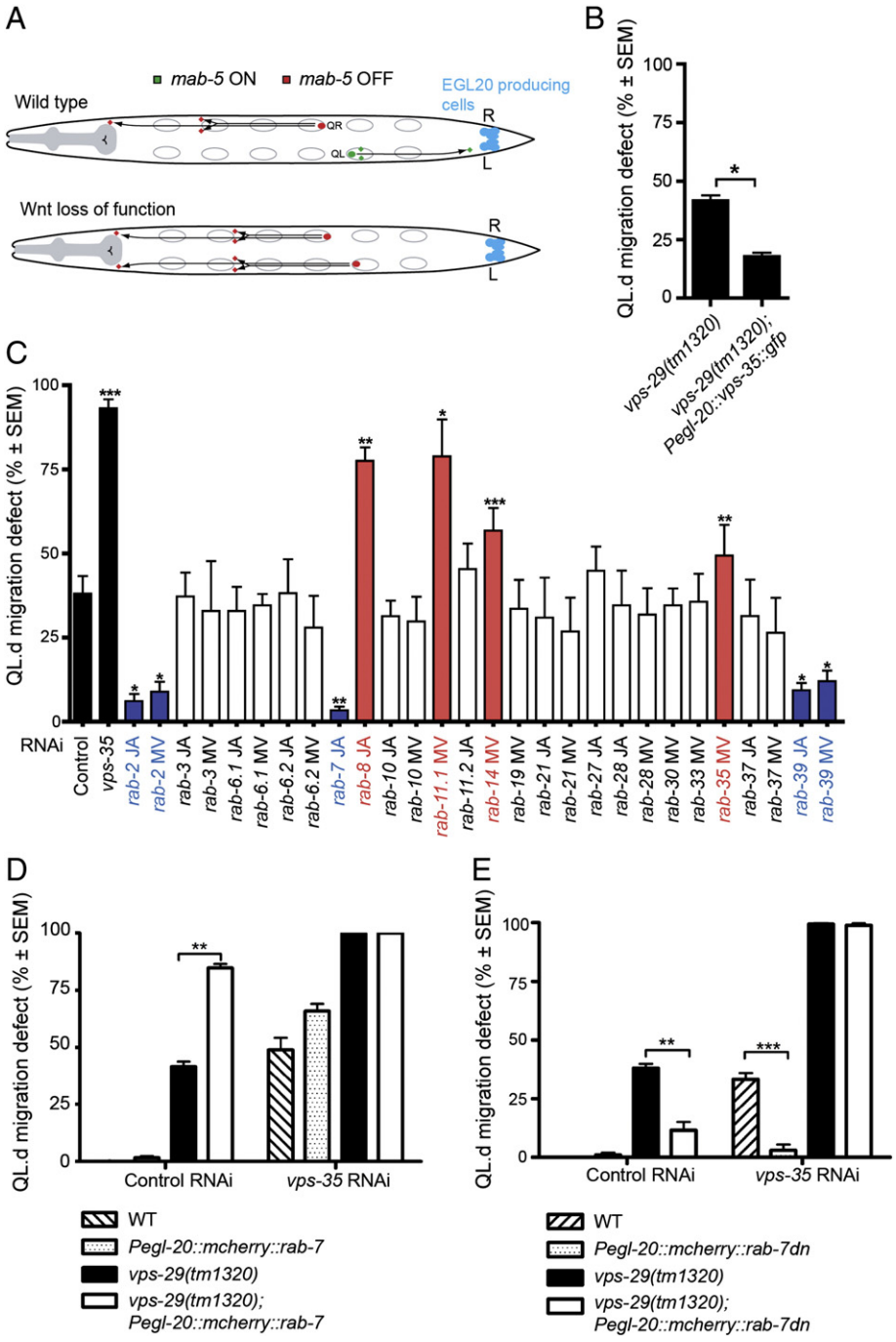


**Fig. 1.** Knock-down of *rab-7* restores EGL-20/Wnt signaling in *vps-29* mutants. (A) Schematic representation of the migration of the Q neuroblast descendants in wild type L1 larvae and in animals with impaired EGL-20/Wnt signaling. Dorsal view. Cells expressing *mab-5* are depicted in green. The *egl-20* expressing cells in the tail are indicated in blue. Gray circles indicate the position of the seam cells V1 to V6. (B) Rescue of the QL.d. migration defect of *vps-29(tm1320)* by overexpression of VPS-35::GFP in EGL-20/Wnt producing cells. (C) RNAi screen for Rab genes that enhance or suppress the *vps-29* induced QL.d migration defect. MV and JA indicate RNAi clones from the Vidal or Ahringer RNAi libraries, respectively [38,39]. Data from at least three independent experiments are presented as mean +/− SEM (in each case, n > 100). * $p < 0.05$; ** $p < 0.01$; ***$p < 0.001$. (D) QL.d migration phenotype of *vps-29* single mutants and *vps-29* mutants overexpressing wild type mCherry::RAB-7 in EGL-20/Wnt producing cells. Animals were treated with control or *vps-35* RNAi. (E) QL.d migration phenotype of *vps-29* single mutants and *vps-29* mutants overexpressing dominant negative (dn) mCherry::RAB-7 in EGL-20/Wnt producing cells. Animals were treated with control or *vps-35* RNAi. mCherry::RAB-7 and mCherry::RAB-7dn were expressed under the control of the *egl-20* promoter from an extra-chromosomal array. Data from at least three independent experiments are presented as mean +/− SEM (in each case, n > 100). ** $p < 0.01$; *** $p < 0.001$.

Of the three cargo-selective subunits of the retromer, null mutations of *vps-35* and *vps-26* induce a fully penetrant defect in QL.d migration, but a null mutation of *vps-29* induces only a partially penetrant defect (Fig. 1B) [12]. This difference is also reflected in the effect of the different cargo-selective subunit mutations on steady state levels of the *C. elegans* Wls ortholog MIG-14, with a strong reduction in MIG-14/Wls protein levels in *vps-35* and *vps-26* mutants, but only an intermediate reduction in *vps-29* mutants [10]. These observations suggest that the retromer dependent retrieval of MIG-14/Wls is only partially disrupted in *vps-29* mutants. Double mutant combinations of *vps-29* with *vps-26* or *vps-35* are synthetic lethal [12], but partial knock-down of *vps-35* in *vps-29* mutants does not interfere with viability. Consistent with a non-essential function of *vps-29* in MIG-14/Wls retrieval, we found that the *vps-29* induced defect in the posterior localization of the QL.d was strongly enhanced by knock-down of *vps-35* (Fig. 1C, D, E) and that the steady state level of a functional MIG-14::GFP fusion protein

expressed at endogenous levels (see below) was strongly reduced by *vps-35* RNAi in *vps-29* mutants (Fig. 8C). Furthermore, we found that QL.d migration was rescued by overexpression of VPS-35 (Fig. 1B), indicating that in the absence of the VPS-29 subunit, retromer function can be restored by adding an excess of the cargo-binding subunit VPS-35. Whether VPS-29 is required for the efficient binding of the Vps26–29–35 trimer to MIG-14/Wls or whether the stability of the retromer complex is reduced in the absence of VPS-29 remains to be established.

### 3.2. Knock-down of rab-7 restores EGL-20/Wnt signaling in vps-29 mutants

To gain further understanding of the mechanism of Wnt secretion and in particular the retromer dependent MIG-14/Wls retrieval step, we used the *vps-29* null mutant as a sensitized genetic background to assay how blocking specific trafficking pathways influences EGL-20/Wnt signaling. In this analysis, we focused on the Rab proteins, a family of small GTPases that function as key regulators of intracellular trafficking [43]. Using available RNAi resources [38,39], we knocked down 19 of the 31 predicted Rab genes of *C. elegans* and found a statistically significant enhancement of the *vps-29* induced QL.d migration defect for *rab-8*, *rab-11.1*, *rab-14* and *rab-35*, while the phenotype was significantly suppressed upon knock-down of *rab-2*, *rab-7* and *rab-39* (Fig. 1C). The function of *rab-1* and *rab-5* could not be addressed, since knock-down of these genes resulted in embryonic lethality.

Rab7 is an important regulator of endosomal maturation, controlling both late endosome formation and the fusion of late endosomes with lysosomes [43]. In addition, Rab7 directly binds the cargo-selective subunit Vps35, an interaction that facilitates recruitment of the mammalian Vps26–29–35 trimer to endosomes and retrograde transport of the CI-MPR [26,27,30]. The suppression of the *vps-29* induced QL.d migration phenotype by knock-down of the *C. elegans* Rab7 ortholog *rab-7* prompted us to further investigate the function of RAB-7 in the retromer dependent recycling of MIG-14/Wls.

### 3.3. RAB-7 acts in EGL-20/Wnt producing cells

To investigate whether *vps-29* and *rab-7* act together in Wnt producing cells, we expressed wild type RAB-7 and dominant negative RAB-7 (RAB-7dn) tagged with mCherry in *egl-20* expressing cells and assayed the EGL-20/Wnt dependent migration of the QL.d in *vps-29* mutant animals. In line with the RNAi results, overexpression of RAB-7dn rescued the *vps-29* induced QL.d migration defect (Fig. 1E), whereas overexpression of wild type RAB-7 enhanced the phenotype (Fig. 1D), consistent with a cell autonomous function of RAB-7 in EGL-20/Wnt producing cells. When retromer function in *vps-29* mutants was further reduced by knock-down of *vps-35*, overexpression of RAB-7dn did not restore posterior QL.d migration, indicating that inhibition of RAB-7 only rescues QL.d migration when the cargo-selective subcomplex of the retromer is still partially functional.

Next, we investigated whether inhibition of RAB-7 rescues QL.d migration by restoring EGL-20/Wnt secretion in *vps-29* mutants. To visualize EGL-20/Wnt, we used a functional fusion of EGL-20 with the immunoglobulin-binding domain of protein A, which forms a punctate concentration gradient that ranges from the *egl-20* expressing cells in the tail to the mid-body region [12,31] (Fig. 2A). Quantification of EGL-20::protA staining showed a clear reduction of the gradient in *vps-35* and *vps-29* mutants (Fig. 2B, C). In line with the notion that retromer function is only partially defective in *vps-29* mutants, the reduction in EGL-20::protA staining was less severe as in *vps-35* mutants (as measured by exponential decay constants, see Materials and methods). Importantly, we found that EGL-20::protA secretion was partially restored in *vps-29* mutants expressing dominant negative RAB-7 (Fig. 2A, E, G), while no rescue was observed in *vps-29* mutants expressing wild type RAB-7 (Fig. 2A, D, F). Taken together, these results demonstrate that inhibition of RAB-7 rescues the EGL-20/Wnt signaling defect of *vps-29* by restoring EGL-20/Wnt secretion.

Overexpression of wild type or dominant negative RAB-7 did not influence QL.d migration in wild type animals (Fig. 1D, E). Consistently, overexpression of wild type or dominant negative RAB-7 did not have a significant effect on the EGL-20::ProtA gradient in a wild type background (Fig. 2A, D, E, F, G), indicating that under normal conditions RAB-7 does not play a major role in EGL-20/Wnt secretion.

### 3.4. Inhibition of RAB-7 increases MIG-14/Wls protein levels in vps-29 mutants

MIG-14/Wls cycles between the Golgi complex and the plasma membrane to mediate Wnt secretion [6–10]. To further investigate how inhibition of RAB-7 restores EGL-20/Wnt secretion in *vps-29* mutants, we tested the effect of wild type or dominant negative RAB-7 on the subcellular localization of MIG-14/Wls in EGL-20/Wnt producing cells. To visualize MIG-14, we generated a functional fusion of MIG-14 with GFP and expressed it at endogenous levels using Mos1 mediated single copy integration (Fig. 3). As shown in Fig. 4A, MIG-14::GFP localizes to intracellular punctae and the cell membrane [10]. Using mCherry::RAB-5 as a marker of early endosomes (Fig. 6A) and mCherry::RAB-7 (Fig. 4A) and LMP-1::mCherry (Fig. 5A) as markers of late endosomes, we found that MIG-14::GFP mostly localizes to early endosomes, as has been reported previously [3,7,9,10]. In *vps-29* mutants, on the other hand, MIG-14::GFP protein levels were reduced (as measured by GFP fluorescence intensity), with most of the remaining protein localizing to mCherry::RAB-7 and LMP-1::mCherry positive late endosomes or lysosomes (Figs. 4A, B and 5A, B) [10]. Expression of dominant negative mCherry::RAB-7dn did not significantly alter the localization and protein levels of MIG-14::GFP in wild type animals, consistent with the observation that RAB-7dn does not affect EGL-20/Wnt secretion and QL.d migration under normal conditions (Fig. 4A, B). In contrast, RAB-7dn induced a punctate accumulation of MIG-14::GFP in *vps-29* mutants (Fig. 4A, B). In the absence of retromer function, MIG-14/Wls enters the lysosomal degradation pathway and steady state protein levels are strongly reduced [7,9,10]. When RAB-7 function is inhibited, the induced block in endosomal maturation may prevent this degradation, leading to accumulation of MIG-14/Wls in maturing endosomes.

### 3.5. Inhibition of late endosomal maturation restores EGL-20/Wnt signaling in vps-29 mutants

To investigate whether inhibition of late endosomal maturation is sufficient to restore Wnt signaling in *vps-29* mutants, we investigated MIG-14/Wls localization and EGL-20/Wnt signaling in *tbc-2* mutants. *tbc-2* encodes a Rab GTPase activating protein (GAP) that shows high activity towards Rab5 [35,44]. TBC-2 colocalizes with Rab7 on late endosomes and is thought to inactivate Rab5 to complete the Rab5 to Rab7 conversion during endosomal maturation [44]. Consistent with these observations, we found that mutation of *tbc-2* leads to the formation of enlarged punctate structures that are positive for the late endosomal and lysosomal marker LMP-1::mCherry (Fig. 5A) [10,44]. To determine the effect of *tbc-2* on MIG-14/Wls trafficking, we analyzed the subcellular localization of MIG-14::GFP in EGL-20/Wnt producing cells. *tbc-2* did not significantly alter the subcellular distribution of MIG-14/Wls in a wild type background, except for a slightly enhanced colocalization with LMP-1::mCherry (Fig. 5A). In *vps-29; tbc-2* double mutants, however, MIG-14::GFP mostly localized to LMP-1::mCherry positive vesicles. Compared to *vps-29* single mutants, there was a significant increase in MIG-14::GFP protein level (Fig. 5B), indicating that mutation of *tbc-2* induces accumulation of MIG-14/Wls in late endosomes. Next, we investigated whether this block in endosomal maturation restores EGL-20/Wnt signaling and secretion. As shown in Fig. 5C, *tbc-2* rescued the QL.d migration phenotype of *vps-29*, whereas overexpression of *tbc-2* in EGL-20/Wnt producing cells strongly enhanced the phenotype. Furthermore, *tbc-2* restored EGL-20/Wnt

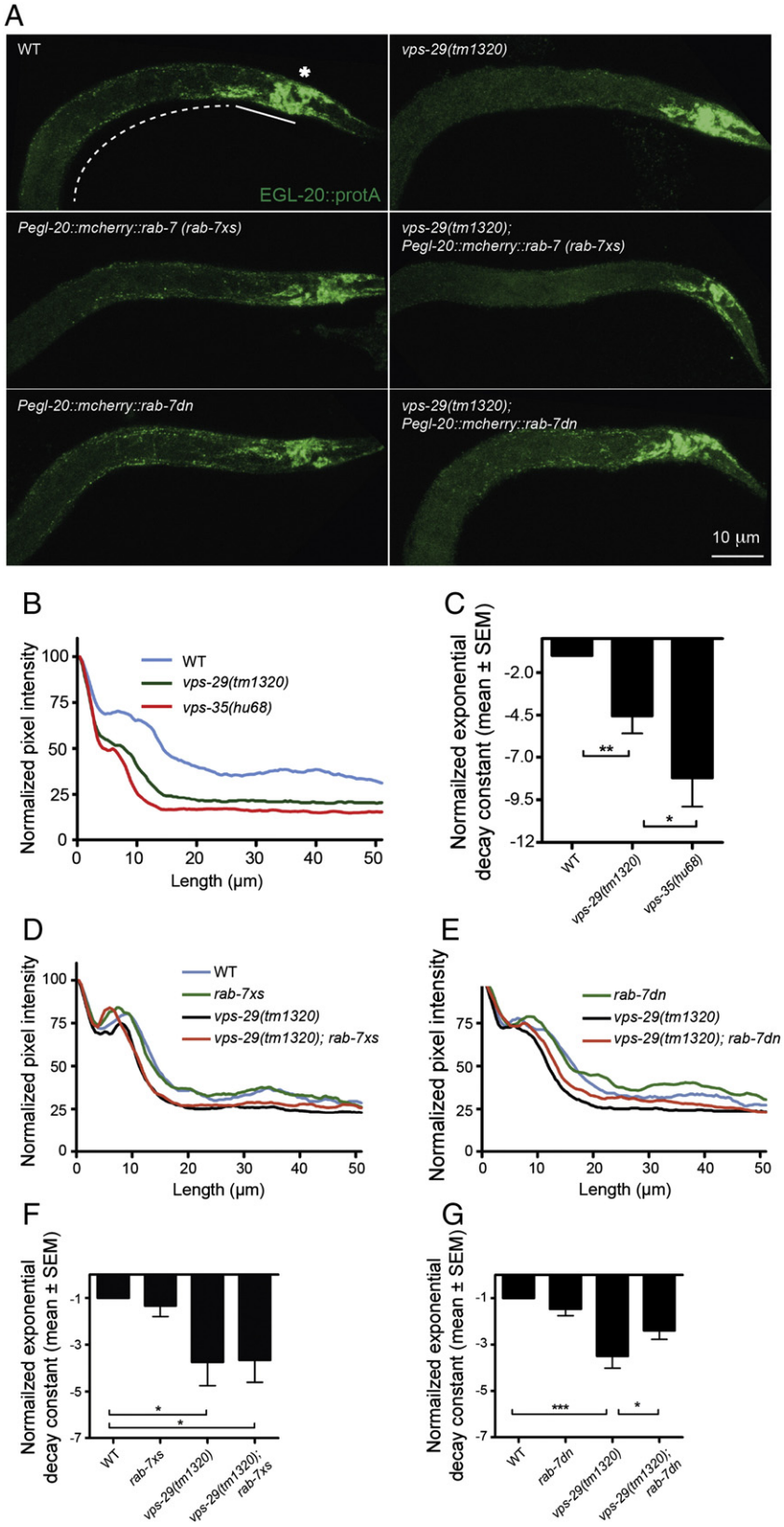


**Fig. 2.** Dominant negative RAB-7 restores EGL-20/Wnt secretion in *vps-29* mutants. (A) Staining of EGL-20::protein A with a rabbit anti-goat-Cy5 antibody in wild type or *vps-29(tm1320)* mutants expressing mCherry::RAB-7 (*rab-7xs*) or mCherry::RAB-7dn in EGL-20/Wnt producing cells. Expression of EGL-20/Wnt is visible in the *egl-20* expressing cells (closed line) and as a punctate posterior to anterior gradient (dotted line). In all images, anterior is to the left and dorsal is up. Images are maximum projections of 10 confocal sections taken at 0.5 µm z-steps. Asterisk indicates the starting point of the quantification shown in D and E. Scale bar is 10 µm. (B, D, E) Quantification of EGL-20::protein A staining along the anteroposterior axis. Data from two independent experiments are presented as mean and normalized to the staining intensity in EGL-20/Wnt producing cells (in each case, n > 15). (C, F, G) Statistical analysis of EGL-20::protein A staining quantified in (B, D, E). Data are presented as mean +/− SEM. * $p < 0.05$, ** $p < 0.01$ (C); * $p < 0.02$, ** $p < 0.005$, *** $p < 0.0001$ (F, G).

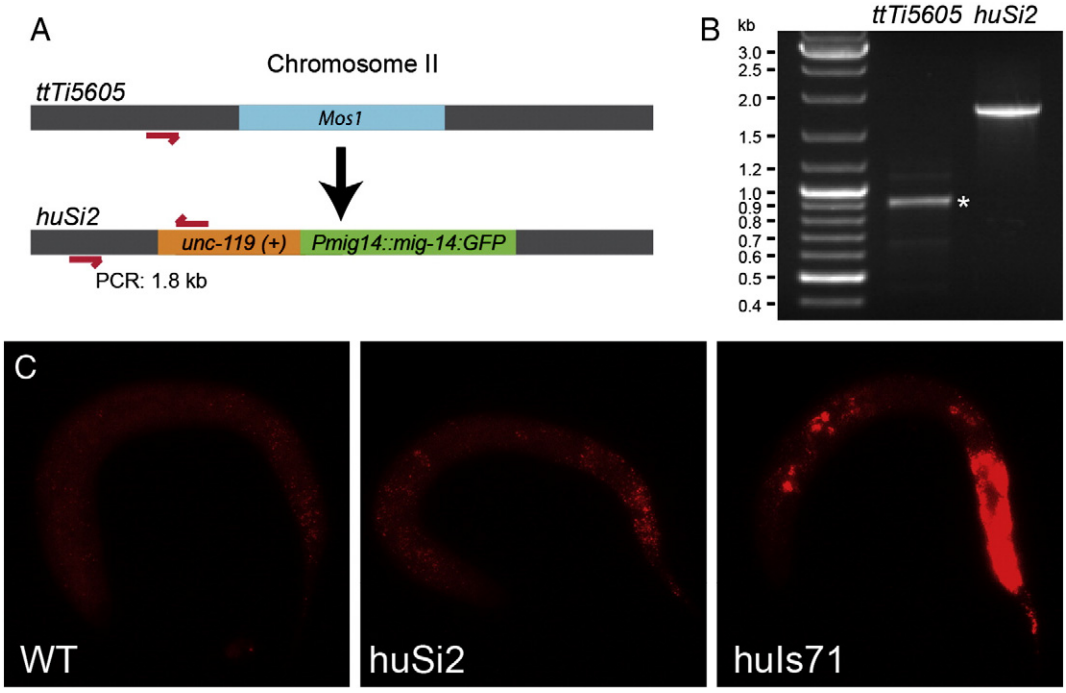


**Fig. 3.** Generation and expression of the single copy *Pmig-14::mig-14::gfp* transgene *huSi2*. (A) Insertion of the transgene at the *ttTi5605* Mos1 integration site [72]. Primers used to detect the insertion are indicated in red. (B) Amplification of the correct 1.8 kb fragment is in *huSi2*. The asterisk indicates a background amplification product in *ttTi5605*. (C) Single mRNA fluorescent in situ hybridization (smFISH) of *mig-14* mRNA in wild type, *huSi2* and the multi-copy integrated *Pmig-14::mig-14::gfp* transgene *huIs71*. Note that the *huSi2* and *huIs71* containing strains also express the endogenous *mig-14* gene.

secretion in *vps-29* mutants (Fig. 5D, E and F). Taken together with the data on dominant negative RAB-7, these results indicate that inhibition of late endosomal maturation restores Wnt signaling in *vps-29* mutants. This conclusion is further supported by our observation that inhibition of the HOPS complex, which binds to activated RAB-7 to coordinate the maturation of late endosomes into lysosomes [45], restores Wnt signaling in *vps-29* mutants as well (Fig. 5G).

In contrast to inhibition of late endosomal maturation, we found that interfering with endosomal maturation at the level of early endosomes did not restore Wnt signaling in *vps-29* mutants. SAND-1 plays a central role in Rab5 to Rab7 conversion and endosomal maturation [36,37,46,47]. SAND-1 is recruited to early endosomes where it binds to and displaces the Rab5 guanine nucleotide exchange factor (GEF) Rabex5 to inhibit Rab5 activity. In addition, it functions at a later stage in the endosomal maturation pathway by interacting with the HOPS complex to activate Rab7 to coordinate the exchange of Rab5 for Rab7 during the Rab5 to Rab7 conversion process. *sand-1* mutants show enlarged Rab5 positive early endosomes in which endocytosed proteins accumulate [46]. We found that MIG-14::GFP showed a more punctate distribution in *sand-1* single and *sand-1; vps-29* double mutants (Fig. 6A). Furthermore, MIG-14::GFP strongly co-localized with the early endosomal marker mCherry::RAB-5. This early endosomal localization was accompanied by a significant increase in MIG-14::GFP protein level in the *sand-1; vps-29* double mutant, consistent with accumulation of MIG-14::GFP in early endosomes (Fig. 6A, B). In contrast to the RAB-7dn and *tbc-2* induced late endosomal accumulation of MIG-14/Wls, accumulation of MIG-14/Wls in early endosomes did not restore EGL-20/Wnt signaling. Instead, we found that mutation of *sand-1* enhanced the *vps-29* induced QL.d migration defect (Fig. 6C), a phenotype that was suppressed by expression of wild type *sand-1* in EGL-20/Wnt producing cells. Furthermore, mutation of *sand-1* alone was sufficient to cause a weak but significant defect in EGL-20/Wnt signaling.

Taken together, these results show that early endosomal maturation is required for the normal trafficking of MIG-14/Wls and that blocking this step interferes with the retrieval of MIG-14/Wls in *vps-29* retromer mutants. This conclusion is further supported by our observation that knock-down of *vps-8*, a subunit of the CORVET complex – which together with RAB-5 is required for the early endosomal localization of SAND-1 [45] – enhances the *vps-29* induced QL.d migration defect as well (Fig. 5G).

SAND-1 functions together with CCZ-1 to control phagosome maturation and engulfment of apoptotic cells in *C. elegans* [36,37]. Interestingly, we found that loss of *ccz-1* did not affect EGL-20/Wnt signaling in a wild type or *vps-29* mutant background (Fig. 6D), indicating that the effect of *sand-1* on MIG-14/Wls trafficking and EGL-20/Wnt signaling is independent of CCZ-1.

### 3.6. Inhibition of ESCRT mediated intraluminal vesicle formation restores EGL-20/Wnt signaling in vps-29 mutants

During endosomal maturation, endocytosed transmembrane proteins such as MIG-14/Wls are internalized and incorporated into intraluminal vesicles (ILVs) (reviewed in [48–50]). The formation of ILVs is mediated by the endosomal-sorting complex required for transport (ESCRT) complex. Depletion of components of the ESCRT machinery results in fewer ILVs and accumulation of endocytosed transmembrane proteins on the limiting endosomal membrane. To test whether inhibition of ILV formation influences the *vps-29* induced EGL-20/Wnt signaling phenotype, we knocked down the ESCRT complex components *vps-28* and *vps-37*. As shown in Fig. 7, knock-down of *vps-28* and *vps-37* rescued the EGL-20/Wnt dependent migration of the QL.d. These results show that inhibition of ILV formation restores Wnt signaling in *vps-29* mutants, either by reducing MIG-14/Wls degradation or by inducing accumulation of MIG-14/Wls on the outer endosomal membrane.

### 3.7. A SNX-BAR dependent retromer pathway contributes to MIG-14/Wls retrieval in vps-29 mutants

We have previously shown that MIG-14/Wls retrieval requires a SNX3 dependent retromer pathway that functions independent of the SNX-BAR retromer sorting nexins SNX1/SNX2 and SNX5/SNX6 [31]. Analysis of the localization of SNX3 along the endosomal maturation

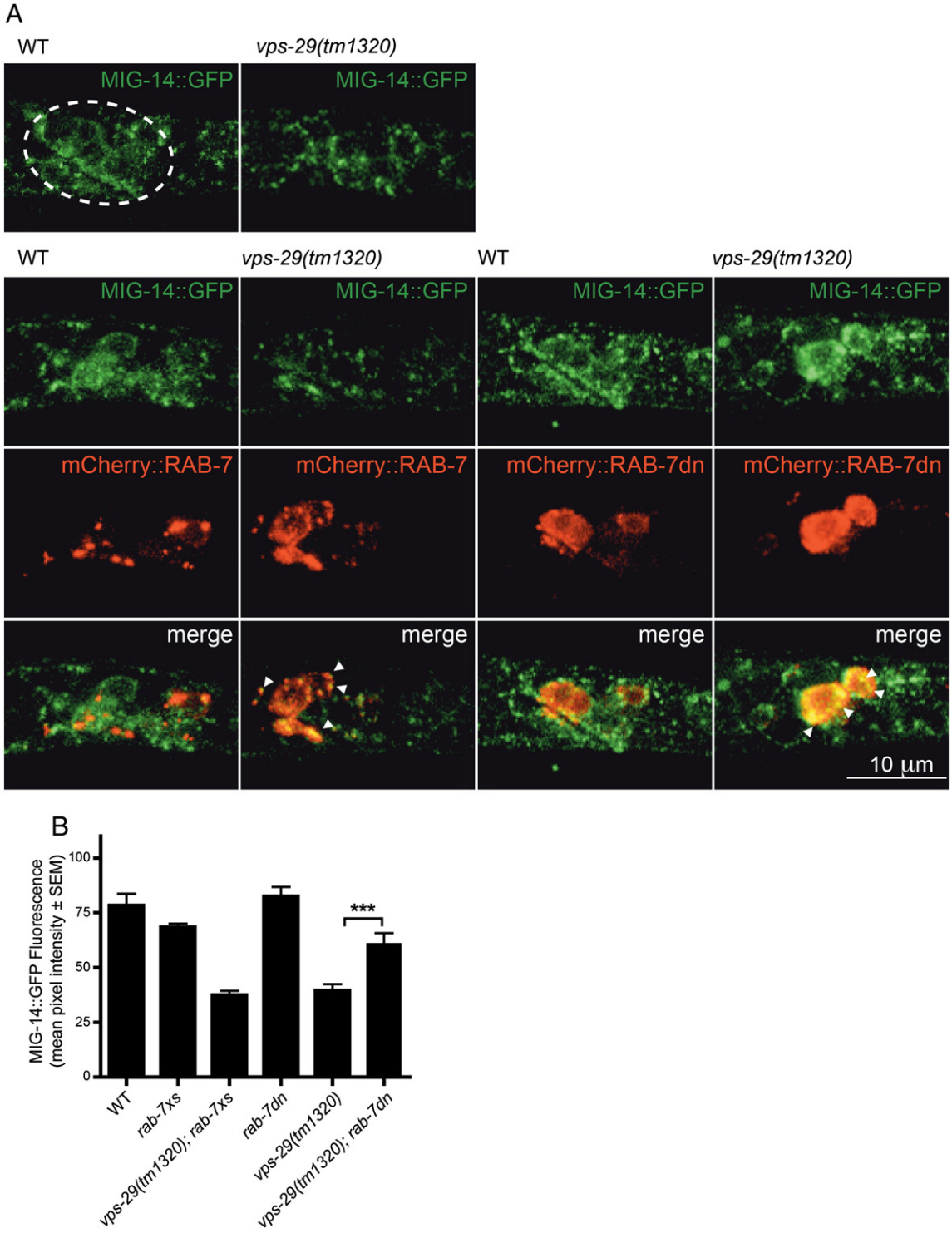


**Fig. 4.** MIG-14/Wls accumulates in the endosomal system in the absence of RAB-7. (A) Localization of MIG-14::GFP in wild type animals and in *vps-29* mutants expressing mCherry::RAB-7 (*rab-7xs*) or dominant negative mCherry::RAB-7dn (*rab-7dn*) in EGL-20/Wnt producing cells. MIG-14::GFP was expressed from its own promoter using the single copy transgene *huSi2*. The L1 stage tail area with the EGL-20/Wnt producing cells is shown. Images are maximum projections of 10 confocal sections taken at 0.25 µm z-steps. Arrow heads indicate examples of co-localization between MIG-14::GFP and mCherry::RAB-7 or vesicular accumulation of MIG-14::GFP in cells expressing dominant negative mCherry::RAB-7dn. Images are representative of three independent experiments. Scale bar is 10 µm. (B) Quantification of the data shown in (A). The dotted oval indicates the region of EGL-20/Wnt producing cells taken for quantification. Data are presented as mean +/− SEM (in each case, n = 10). *** $p < 0.0001$.

pathway has shown that SNX3 is enriched on early endosomes [31], while the SNX-BAR sorting nexins SNX1/SNX2 and SNX5/SNX6 are more abundant on endosomes that are at the early-to-late transition point [28,29]. Based on these observations, we hypothesized that a reduction in the SNX3 retromer-mediated retrieval of MIG-14/Wls from early endosomes in *vps-29* mutants might lead to retrieval of MIG-14/Wls from more mature endosomes through a SNX-BAR retromer dependent pathway. To investigate this possibility, we removed *snx-3* or the SNX-BAR sorting nexin *snx-1* from *vps-29* mutants and assayed effects on the EGL-20/Wnt dependent migration of the QL.d. In line with the essential function of the SNX-3 retromer pathway in MIG-14/Wls recycling [31], loss of *snx-3* induced a fully penetrant defect in QL.d

migration, while knock-down or mutation of *snx-1* had no effect on EGL-20/Wnt signaling in wild type animals (Fig. 8A, B). However, knock-down of *snx-1* strongly enhanced the QL.d migration defect of *vps-29* (Fig. 8B). Furthermore, we found that the steady state level of MIG-14::GFP in *vps-29* mutants was strongly reduced by *snx-1* RNAi (Fig. 8C), indicating that in the absence of *vps-29*, MIG-14/Wls retrieval

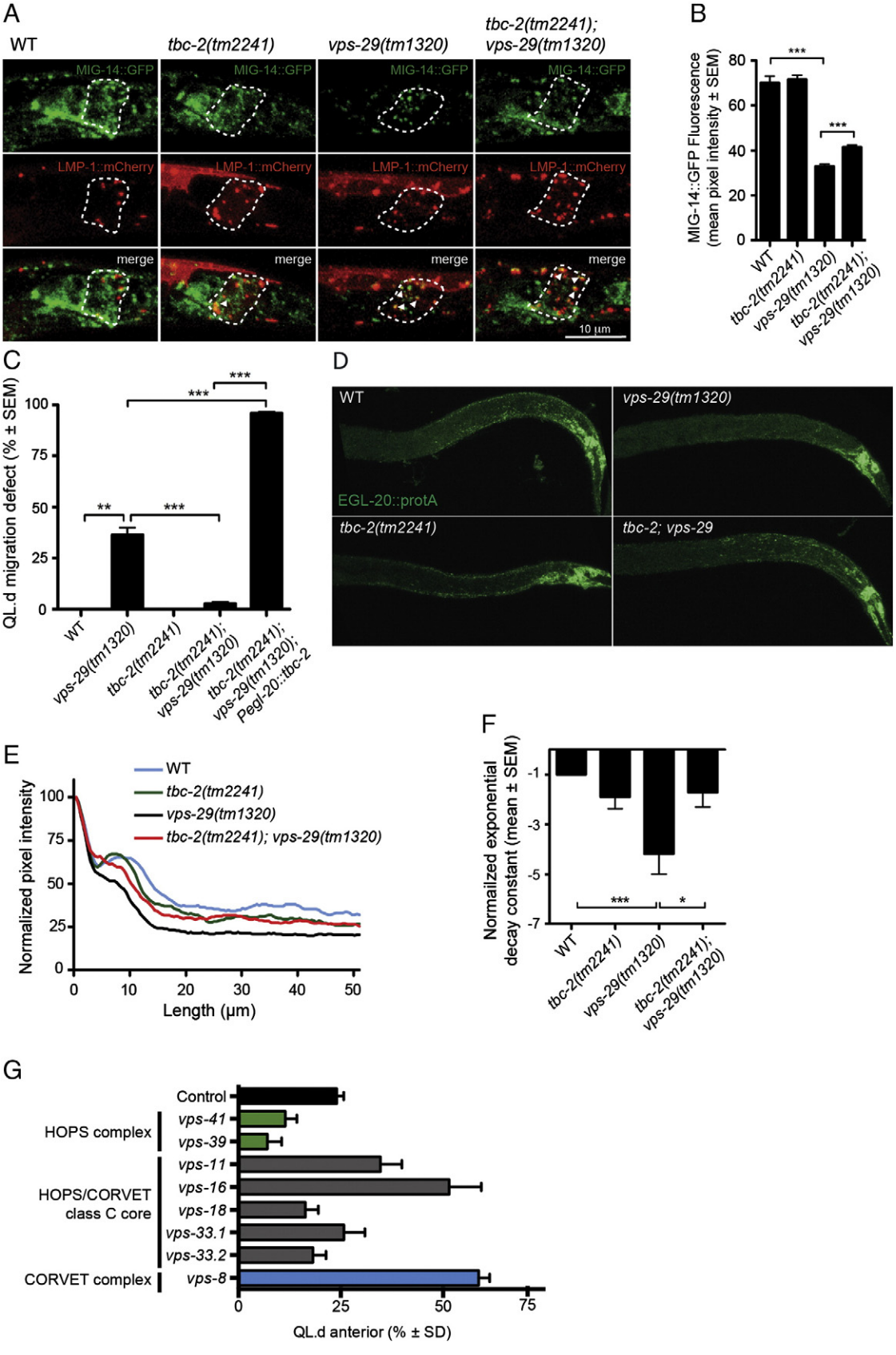

is partially dependent on the SNX-BAR retromer pathway. Next, we investigated whether *snx-1* is required for the RAB-7dn dependent rescue of EGL-20/Wnt signaling. Whereas RAB-7dn restored posterior QL.d migration in *vps-29* mutants treated with control RNAi, there was no significant reduction in the QL.d migration defect in animals treated with *snx-1* RNAi (Fig. 8B), indicating that the rescuing activity of RAB-7dn is also dependent on SNX-BAR retromer function. Taken together, these results are consistent with a model in which the incomplete retrieval of MIG-14/Wls by the SNX-3 retromer pathway in *vps-29* mutants can be compensated by blocking endosomal maturation and partial retrieval of MIG-14/Wls from late endosomes through a SNX-BAR dependent retromer pathway.

## 4. Discussion

The identification of the Wnt sorting receptor MIG-14/Wls and the retromer complex as key regulators of Wnt secretion has demonstrated that Wnt is released through a specialized secretion mechanism that provides an important layer of control to the Wnt signaling pathway [3–9,11,12]. MIG-14/Wls is a direct cargo of the retromer complex, which functions as part of a transport route that retrieves MIG-14/Wls from the plasma membrane to the TGN. We have recently shown that the retromer dependent retrieval of MIG-14/Wls is mediated by an alternative retromer pathway that is dependent on the sorting nexin SNX3 instead of the classical SNX-BAR retromer sorting nexins SNX1/SNX2 and SNX5/SNX6 [31]. In this study, we have further investigated the retromer dependent endosome-to-TGN retrieval of MIG-14/Wls. We demonstrate that the retrieval of MIG-14/Wls is partially disrupted in mutants of the *C. elegans* retromer subunit gene *vps-29* and that it can be restored by blocking the maturation of late endosomes to lysosomes. This results in accumulation of MIG-14/Wls in a late endosomal compartment from which MIG-14/Wls can be partially retrieved through a SNX-BAR dependent retromer pathway.

### 4.1. Mutation of vps-29 partially disrupts the retromer dependent recycling of MIG-14/Wls

The cargo-selective subcomplex of the retromer consists of the subunits Vps26, Vps29 and Vps35. Structural analysis of the cargo-selective subcomplex has shown that Vps26 and Vps29 bind to independent sites on Vps35, the subunit that directly interacts with cargo proteins such as Sortilin and the CI-MPR [51–53]. As part of this complex, Vps26 has been shown to promote membrane association of the cargo-selective subcomplex, while Vps29 is thought to stabilize the interaction with the SNX-BAR sorting nexins [52–55]. In *C. elegans*, VPS-26 and VPS-35 are essential for the retromer dependent recycling of MIG-14/Wls, while our results show that VPS-29 plays a less important role, with *vps-29* mutants showing only a partial reduction in MIG-14/Wls levels and EGL-20/Wnt secretion [10]. This is in contrast to the function of Vps29 in mammalian cells, where knock-down of Vps29 destabilizes the cargo-selective subcomplex [56]. However, in yeast, Vps35p and Vps26p can still interact in the absence of Vps29p, albeit at reduced levels [57]. Furthermore, the stability of Vps35p, but not Vps26p, is decreased in yeast *Vps29* mutants [54]. Our results demonstrate that overexpression of the VPS-35 subunit restores Wnt signaling in *vps-29* mutants. This is in line with a less stable and partially functional cargo-selective subcomplex, a defect that can be compensated by an excess of the cargo-binding VPS-35 subunit. In the context of EGL-20/Wnt secretion, the effect of *vps-29* mutation may therefore be similar as loss of Vps29p in yeast.

### 4.2. A screen for Rab GTPases that suppress or enhance the Wnt signaling phenotype of vps-29

Rab GTPases are important regulators of vesicle trafficking [43]. In our screen, we found that knock-down of *rab-8*, *rab-11.1*, *rab-14* and *rab-35* enhanced the Wnt signaling phenotype of *vps-29*. Interestingly, all of these Rabs have been shown to function at the level of the recycling endosome, indicating that retrieval from this compartment could contribute to the trafficking of endocytosed MIG-14/Wls and the regulation of Wnt secretion. In addition, Rab8 has been shown to be required for basolateral secretion [58–62], while Rab35 has been implicated in exosome formation [63]. This latter function is of particular interest, as recent evidence suggests that Wls and Wnt can be secreted on exosomes [64,65]. Rab GTPases that suppressed the Wnt signaling phenotype of *vps-29* include *rab-2*, *rab-7* and *rab-39*. These Rabs have been implicated in early-to-late endosome maturation, the conversion of late endosomes into lysosomes and phagosome maturation [43,66,67].

### 4.3. Function of RAB-7 in the retromer-dependent retrieval of MIG-14/Wls

It has recently been shown that Rab7 interacts with the cargo-selective Vps35 subunit of the Vps26–29–35 trimer, a function that is required to facilitate recruitment of the cargo-selective subcomplex to endosomal membranes and retrograde trafficking of the CI-MPR [26,27,30]. We found that inhibition of the *C. elegans* Rab7 ortholog RAB-7 did not interfere with MIG-14/Wls recycling or Wnt secretion, as assayed by the effect on EGL-20/Wnt signaling and gradient formation. Moreover, inhibition of RAB-7 rescued EGL-20/Wnt secretion in *vps-29* mutants. Under these conditions, MIG-14/Wls accumulates in late endosomes, from which it can be partially retrieved through a SNX-BAR dependent retromer pathway. In the context of MIG-14/Wls retrieval, the main function of RAB-7 therefore appears to be its role in endosome maturation. Consistently, we found that overexpression of RAB-7, which promotes endosomal maturation and lysosomal degradation, enhanced the Wnt signaling defect of *vps-29* mutants. Is RAB-7 also required for endosomal recruitment of the *C. elegans* Vps26–29–35 trimer? As *rab-7* null mutants are not viable, we used *rab-7* RNAi and tissue-specific overexpression of dominant negative RAB-7 to partially interfere with RAB-7 function. It is therefore possible that under these conditions sufficient RAB-7 activity remains to mediate its function in retromer recruitment.

Another important aspect of Rab7 function in retromer recruitment is the interaction of Vps29 with the Rab7 GTPase activating protein TBC1D5 [27,68]. By recruiting TBC1D5, Vps29 is thought to inactivate Rab7, triggering dissociation of the cargo-selective Vps26–29–35 trimer

**Fig. 5.** Inhibition of endosome maturation at the level of late endosomes restores EGL-20/Wnt signaling in *vps-29* mutants. (A) Localization of MIG-14::GFP expressed from its own promoter using the single copy transgene *huSi2* in wild type, *tbc-2(tm2241)*, *vps-29(1320)* and *tbc-2(tm2241); vps-29(1320)* animals. The L1 stage tail area with the EGL-20/Wnt producing cells is shown. Images are maximum projections of 10 confocal sections taken at 0.25 μm z-steps. Arrowheads indicate vesicular localization of MIG-14::GFP and examples of co-localization between MIG-14::GFP and LMP-1::mCherry [10]. Images are representative of three independent experiments. Scale bar, 10 μm. (B) Quantification of the data shown in (E). The region taken for quantification was the same as in Fig. 3. Data are presented as mean +/− SEM (in each case, n = 10). *** $p < 0.0001$. (C) Rescue of the QL.d migration phenotype of *vps-29* mutants by *tbc-2(tm2241)* and of the phenotype by *egl-20* promoter directed overexpression of *tbc-2*. Data from at least three independent experiments are presented as mean +/− SEM (in each case, n > 150). ** $p < 0.01$; *** $p < 0.001$. (D) Staining of EGL-20::protein A with a rabbit anti-goat-Cy5 antibody in wild type, *vps-29(tm1320)*, *tbc-2(tm2241)* and *vps-29(tm1320); tbc-2(tm2241)*. In all images, anterior is to the left and dorsal is up. Images are maximum projections of 10 confocal sections taken at 0.5 μm z-steps. (E) Quantification of EGL-20::protein A staining. Data from two independent experiments are presented as mean and normalized to the staining intensity in EGL-20/Wnt producing cells (in each case, n > 20). (F) Statistical analysis of EGL-20::protein A staining quantified in (E). Data are presented as mean +/− SEM. ** $p < 0.03$, *** $p < 0.001$. (G) Knock-down of HOPS complex components (*vps-39* and *vps-41*) suppresses and knock-down of the CORVET complex component *vps-8* enhances the Wnt signaling defect of *vps-29* mutants. Data from at least three independent experiments are presented as mean +/− SD (in each case, n > 100).

from the endosomal membrane. A possibility is therefore that in *vps-29* mutants the TBC1D5 ortholog RBG-3 is not recruited to the retromer complex, leading to excessive RAB-7 activity, premature endosome maturation and MIG-14/Wls degradation. This possibility can however be excluded as *rbg-3* null mutants do not show a defect in EGL-20/Wnt signaling (Fig. 9).

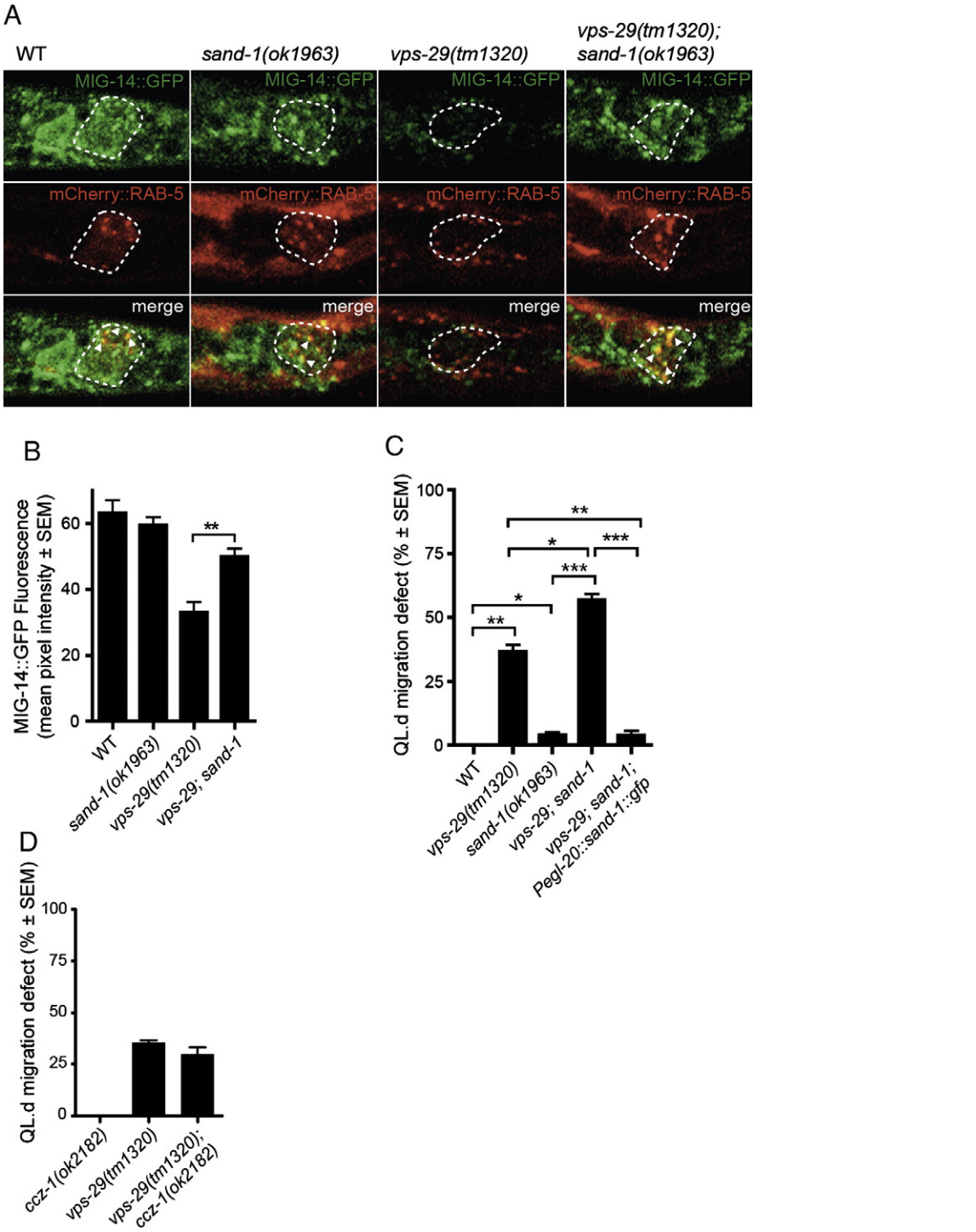


**Fig. 6.** Disruption of early endosome maturation interferes with MIG-14/Wls recycling. (A) Localization of MIG-14::GFP expressed from its own promoter using the single copy transgene *huSi2* in wild type, *sand-1(tm1963)*, *vps-29(tm1320)* and *vps-29(tm1320); sand-1(tm1963)* animals. The L1 stage tail area with the EGL-20/Wnt producing cells is shown. Images are maximum projections of 10 confocal sections taken at 0.25 μm z-steps. Arrowheads indicate vesicular localization of MIG-14::GFP and examples of co-localization between MIG-14::GFP and mCherry::RAB-5 (expressed from the muscle specific myo-3 promoter). Images are representative of three independent experiments. (B) Quantification of the data shown in (A). The region taken for quantification was the same as in Fig. 3. Data are presented as mean +/− SEM (in each case, n = 10). ** $p < 0.01$. (C) QL.d migration phenotype of *sand-1(ok1963)*, *vps-29(tm1320)* and the double mutant, and rescue of the QL.d migration phenotype of *vps-29(1320); sand-1(ok1963)* by expression of *sand-1::gfp* under the control of the *egl-20* promoter. Data from at least four independent experiments are presented as mean +/− SEM (in each case, n > 100). * $p < 0.03$; ** $p < 0.01$; *** $p < 0.001$. (D) *ccz-1* is not required for EGL-20/Wnt signaling. QL.d migration phenotype of *ccz-1(ok2182)*, *vps-29(tm1320)* and *ccz-1(ok2182); vps-29(tm1320)*. Data from at least three independent experiments are presented as mean +/− SEM (in each case, n > 100).

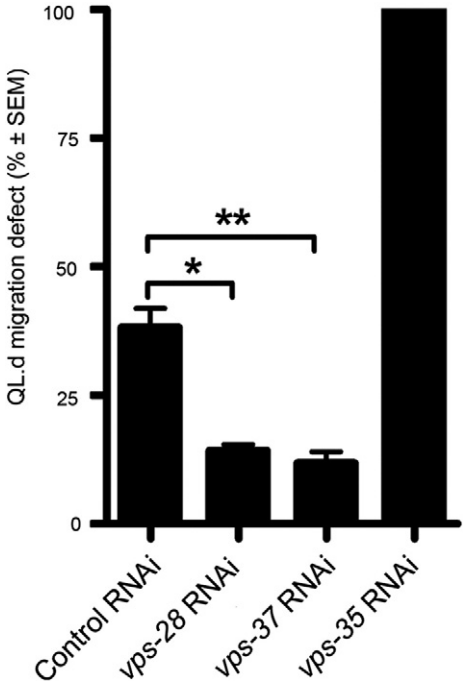


**Fig. 7.** Inhibition of ESCRT components restores EGL-20/Wnt signaling in *vps-29* mutants. *vps-29(tm1320)* animals were treated with control, *vps-28*, *vps-37* or *vps-35* RNAi and the final position of the QL.d was determined. Data from at least three independent experiments are presented as mean +/− SEM (in each case, n > 100). * $p < 0.05$, ** $p < 0.01$.

### 4.4. Inhibition of late endosomal maturation restores EGL-20/Wnt signaling in vps-29 mutants

We found that inhibition of endosomal maturation by *rab-7* RNAi or overexpression of dominant negative RAB-7 rescued EGL-20/Wnt secretion and signaling in *vps-29* mutants. To further investigate how endosomal maturation influences the *vps-29* induced EGL-20/Wnt signaling phenotype, we interfered with endosomal maturation using mutations in *tbc-2* and *sand-1*. MIG-14/Wls accumulated in LMP-1::mCherry positive late endosomes in *tbc-2* mutants. Similar to inhibition of RAB-7, the *tbc-2* induced block in endosomal maturation was sufficient to rescue EGL-20/Wnt secretion and signaling, supporting the model that accumulation of MIG-14/Wls in late endosomes partially restores endosome-to-TGN retrieval of MIG-14/Wls in *vps-29* mutants.

Mutation of *sand-1* resulted in early endosomal accumulation of MIG-14/Wls, an effect that is in agreement with the function of SAND-1 in early to late endosomal maturation [36,37,46,47]. In contrast to late endosomal accumulation, we found that early endosomal accumulation of MIG-14/Wls enhanced the EGL-20/Wnt signaling phenotype of *vps-29*. Furthermore, *sand-1* single mutants displayed a weak but significant defect in EGL-20/Wnt signaling, indicating that loss of *sand-1* not only alters the progression of MIG-14/Wls from early to late endosomes, but also partially interferes with the SNX-3 retromer dependent retrieval of MIG-14/Wls. Taken together with the observations on late endosomal maturation discussed above, these results are consistent with a model in which the retromer dependent retrieval of MIG-14/Wls can take place at both early and late endosomes in *vps-29* mutants.

SAND-1 has been reported to form a complex with CCZ-1. Together, SAND-1 and CCZ-1 regulate endosome maturation by modulating the

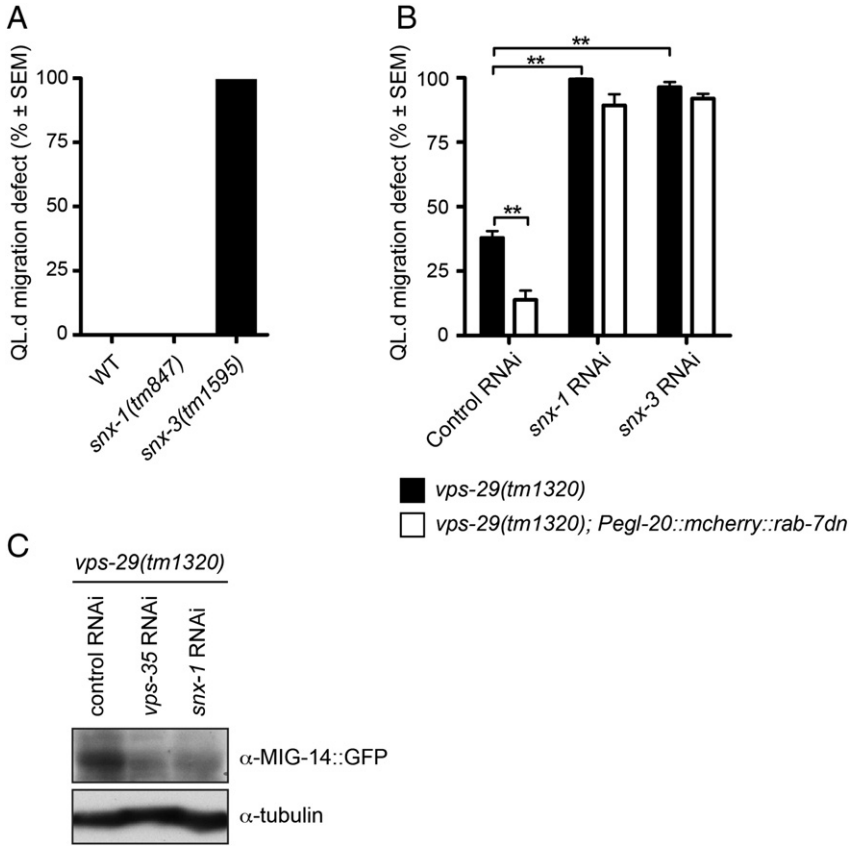


**Fig. 8.** EGL-20/Wnt signaling is dependent on both SNX3 and SNX-BAR retromer pathways in *vps-29* mutants. (A) QL.d migration phenotype of *snx-1* and *snx-3* mutants. Data from at least three independent experiments are presented as mean +/− SEM (n > 100). (B) QL.d migration defect of *vps-29* single mutants and *vps-29* mutants expressing dominant negative mCherry::RAB-7dn in EGL-20/Wnt producing cells. Animals were treated with control, *snx-1* or *snx-3* RNAi. Dominant negative mCherry::RAB-7 was expressed under the control of the *egl-20* promoter from an extra-chromosomal array. Data from at least three independent experiments are presented as mean +/− SEM (in each case, n > 100). ** $p < 0.01$. (C) Western blot of MIG-14::GFP (*huSi2*) from *vps-29(tm1320)* L1 larvae treated with control, *vps-35* or *snx-1* RNAi.

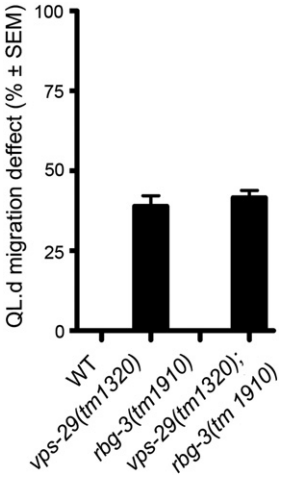


**Fig. 9.** *rbg-3* is not required for EGL-20/Wnt signaling. QL.d migration phenotype of *rbg-3(tm1910)*, *vps-29(tm1320)* and *vps-29(tm1320); rbg-3(tm1910)*. Data from at least three independent experiments are presented as mean +/− SEM (in each case, n > 100).

conversion of Rab5 to Rab7, with SAND-1 controlling the inactivation of RAB-5 and the SAND-1/CCZ-1 complex mediating activation of RAB-7 [36,37,46,47]. The SAND-1/CCZ-1 complex also regulates phagosomal maturation and clearance of apoptotic cells in *C. elegans*. We found that in contrast to *sand-1*, neither *ccz-1* single mutants nor *vps-29; ccz-1* double mutants displayed defects in EGL-20/Wnt signaling, indicating that *sand-1* acts independent of *ccz-1* with respect to MIG-14/Wls retrieval and EGL-20/Wnt secretion.

### *4.5. Spatial separation of SNX-3 and SNX-BAR retromer complexes and cargo-specific mechanisms in MIG-14/Wls retrieval*

The retromer dependent endosome-to-TGN retrieval of cargo proteins such as Sortilin and the CI-MPR is mediated through the classical SNX-BAR retromer pathway, while retrieval of MIG-14/Wls requires an alternative SNX3 dependent retromer pathway [31]. As both pathways utilize the Vps26–29–35 trimer for cargo binding, an important question is how cargo specificity is achieved. One possibility is that the SNX3 and SNX-BAR retromer complexes are differentially localized along the endosomal maturation pathway [24]. Although there is considerable overlap between the localization of SNX3 and the SNX-BAR sorting nexin SNX1 in human cells, SNX3 predominantly localizes to early endosomes, while SNX1 shows a more widespread distribution that includes both early and late endosomes [28,29,31]. Despite this wider distribution, the majority of SNX1 decorated tubules are formed at early-to-late endosomes [29], a stage at which also the SNX-BAR retromer dependent retrieval of Sortilin has been shown to take place [28]. Our previous observations and the results presented in this study demonstrate that SNX-3 is essential for MIG-14/Wls recycling [31]. However, we also show that in *vps-29* mutants, EGL-20/Wnt signaling is dependent on SNX-1, indicating that under these conditions, MIG-14/Wls retrieval can be partially mediated through a SNX-BAR dependent retromer pathway. Indeed, this pathway is required for the RAB-7dn mediated rescue of EGL-20/Wnt signaling in *vps-29* mutants, supporting the notion that accumulation of MIG-14/Wls in late endosomes facilitates retrieval of MIG-14/Wls through a SNX-BAR dependent retromer pathway. Although we cannot rule out a role for SNX-1 in the retrieval of MIG-14/Wls from early endosomes, the more prominent localization of SNX3 on early endosomes [31,69–71] and the requirement of SNX-1 for MIG-14/Wls retrograde trafficking from late endosomes suggest that the SNX-3 and SNX-1 dependent retromer pathways act sequentially in MIG-14/Wls retrieval in *vps-29* mutants. Our results therefore favor a model in which the inefficient recycling of MIG-14/Wls from early endosomes by the SNX-3 retromer pathway in *vps-29* mutants leads to progression of MIG-14/Wls to late endosomes, from which it is retrieved through a SNX-BAR dependent retromer pathway (Fig. 10). Blocking endosomal maturation at the late endosomal stage by interfering with RAB-7 or TBC-2, or preventing internalization of MIG-14/Wls on ILVs by ESCRT knock-down facilitates

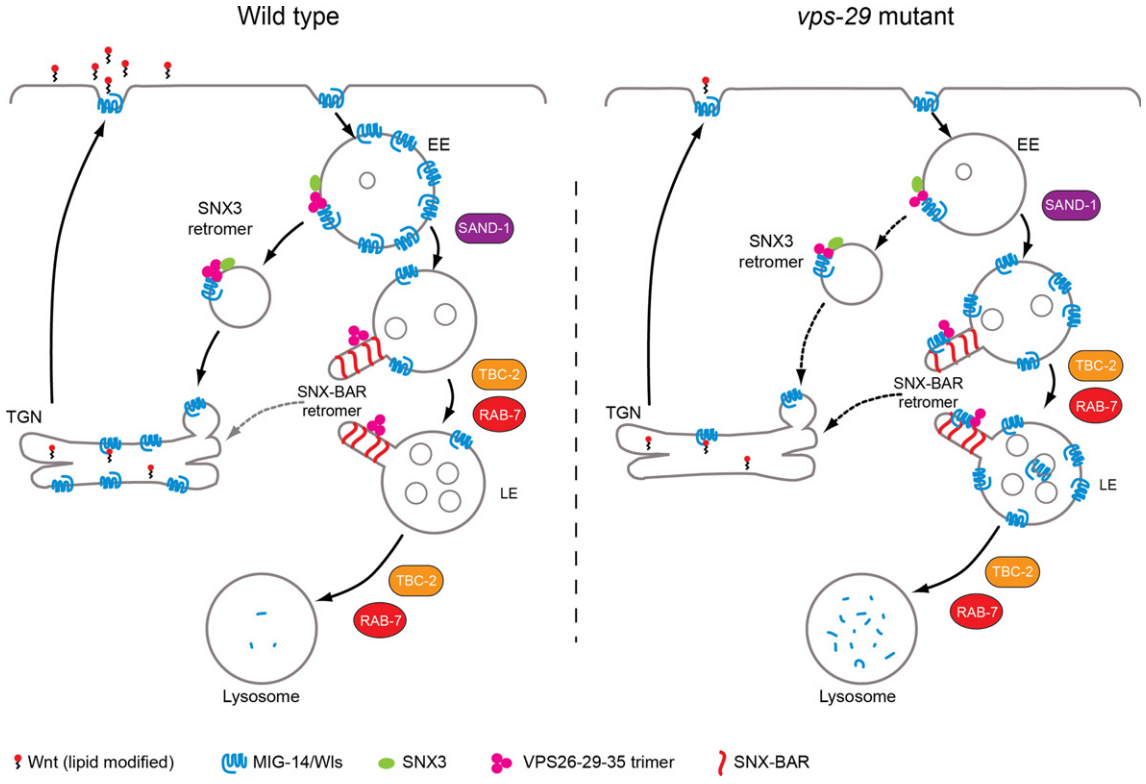


**Fig. 10.** Model of MIG-14/Wls retrieval in wild type and *vps-29* mutants. See text for discussion.

retrieval of MIG-14/Wls through this pathway, leading to a partial restoration of EGL-20/Wnt secretion and signaling in *vps-29* mutants.

How does this model explain the essential function of the SNX-3 retromer pathway in MIG-14/Wls retrieval? We propose that endocytosed MIG-14/Wls first encounters the early endosomal SNX-3 retromer complex, which mediates TGN retrieval of the bulk of MIG-14/Wls that enters the endosomal system. In the absence of the SNX-3 retromer pathway, MIG-14/Wls is retained in the endosomal system and will be a target of the SNX-BAR retromer pathway once the endosomes have matured to the early-to-late endosomal transition point. The entry of endocytosed MIG-14/Wls into early endosomes – as opposed to classical retromer cargo proteins such as Sortilin and the CI-MPR, which enter at a later stage in the endosomal maturation pathway – may therefore be an important factor in determining retrieval through the spatially separated SNX3 and SNX-BAR retromer pathways (Fig. 10). The pool of MIG-14/Wls that can be retrieved through the SNX-BAR retromer pathway is however insufficient to allow normal EGL-20/Wnt secretion in *snx-3* mutants. A major fraction of MIG-14/Wls may already be internalized on ILVs once it reaches the early-to-late endosomal transition point and may therefore be inaccessible to SNX-BAR retromer dependent retrieval. Alternatively, MIG-14/Wls may be a poor substrate of the SNX-BAR retromer pathway. In favor of this latter possibility is our observation that inhibition of ILV formation by knock-down of ESCRT components does not restore EGL-20/Wnt signaling in *snx-3* mutants (data not shown). We therefore propose that in addition to spatial separation of the SNX3 and SNX-BAR retromer complexes, also cargo-specific mechanisms contribute to the specific retrieval of MIG-14/Wls through the SNX3 retromer pathway. This functional separation of retrieval mechanisms may ensure the tight regulation of Wls stability and Wnt secretion that is essential for normal development and adult tissue homeostasis.

## Acknowledgments

We thank Dr. Peter Cullen for critically reading the manuscript, Dr. Wojciech Zajdel for invaluable help in quantification of EGL-20 gradients, Dr. Shohei Mitani (National Bioresource Project for the Nematode, Tokyo, Japan) for deletion mutants, Dr. Andrew Fire for expression vectors and the *Caenorhabditis* Genetic Center (University of Minnesota, Minneapolis) for strains. This work was funded by the Dutch Cancer Society (HUBR 2008-4114), the EU FP6 Program Cells into Organs, an NWO VIDI fellowship (016.076.317) (H.C.K.), an NWO VENI fellowship (M.J.L.), a Boehringer Ingelheim Foundation fellowship (M.H.) and the Grant Agency of the Czech Republic (GACR P305/10/0507) (M.M.).

## References

[1] K.M. Cadigan, R. Nusse, Genes Dev. 11 (1997) 3286–3305.
[2] M. Zecca, K. Basler, G. Struhl, Cell 87 (1996) 833–844.
[3] C. Banziger, D. Soldini, C. Schutt, P. Zipperlen, G. Hausmann, K. Basler, Cell 125 (2006) 509–522.
[4] K. Bartscherer, N. Pelte, D. Ingelfinger, M. Boutros, Cell 125 (2006) 523–533.
[5] R.M. Goodman, S. Thombre, Z. Firtina, D. Gray, D. Betts, J. Roebuck, E.P. Spana, E.M. Selva, Development 133 (2006) 4901–4911.
[6] C.L. Pan, P.D. Baum, M. Gu, E.M. Jorgensen, S.G. Clark, G. Garriga, Dev. Cell 14 (2008) 132–139.
[7] T.Y. Belenkaya, Y. Wu, X. Tang, B. Zhou, L. Cheng, Y.V. Sharma, D. Yan, E.M. Selva, X. Lin, Dev. Cell 14 (2008) 120–131.
[8] X. Franch-Marro, F. Wendler, S. Guidato, J. Griffith, A. Baena-Lopez, N. Itasaki, M.M. Maurice, J.P. Vincent, Nat. Cell Biol. 10 (2008) 170–177.
[9] F. Port, M. Kuster, P. Herr, E. Furger, C. Banziger, G. Hausmann, K. Basler, Nat. Cell Biol. 10 (2008) 178–185.
[10] P.T. Yang, M.J. Lorenowicz, M. Silhankova, D.Y. Coudreuse, M.C. Betist, H.C. Korswagen, Dev. Cell 14 (2008) 140–147.
[11] B.C. Prasad, S.G. Clark, Development 133 (2006) 1757–1766.
[12] D.Y. Coudreuse, G. Roel, M.C. Betist, O. Destree, H.C. Korswagen, Science 312 (2006) 921–924.
[13] C.N. Arighi, L.M. Hartnell, R.C. Aguilar, C.R. Haft, J.S. Bonifacino, J. Cell Biol. 165 (2004) 123–133.
[14] C.R. Haft, M. de la Luz Sierra, R. Bafford, M.A. Lesniak, V.A. Barr, S.I. Taylor, Mol. Biol. Cell 11 (2000) 4105–4116.
[15] M.N. Seaman, J.M. McCaffery, S.D. Emr, J. Cell Biol. 142 (1998) 665–681.
[16] N. Attar, P.J. Cullen, Adv. Enzyme Regul. 50 (2009) 216–236.
[17] T. Wassmer, N. Attar, M. Harterink, J.R. van Weering, C.J. Traer, J. Oakley, B. Goud, D.J. Stephens, P. Verkade, H.C. Korswagen, et al., Dev. Cell 17 (2009) 110–122.
[18] M.N. Seaman, Trends Cell Biol. 15 (2005) 68–75.
[19] M.N. Seaman, J. Cell Sci. 120 (2007) 2378–2389.
[20] M. Tabuchi, I. Yanatori, Y. Kawai, F. Kishi, J. Cell Sci. 123 (2010) 756–766.
[21] J. Carlton, M. Bujny, B.J. Peter, V.M. Oorschot, A. Rutherford, H. Mellor, J. Klumperman, H.T. McMahon, P.J. Cullen, Curr. Biol. 14 (2004) 1791–1800.
[22] J. Carlton, M. Bujny, A. Rutherford, P. Cullen, Traffic 6 (2005) 75–82.
[23] T. Wassmer, N. Attar, M.V. Bujny, J. Oakley, C.J. Traer, P.J. Cullen, J. Cell Sci. 120 (2007) 45–54.
[24] P.J. Cullen, H.C. Korswagen, Nat. Cell Biol. 14 (2012) 29–37.
[25] J. Rink, E. Ghigo, Y. Kalaidzidis, M. Zerial, Cell 122 (2005) 735–749.
[26] R. Rojas, T. van Vlijmen, G.A. Mardones, Y. Prabhu, A.L. Rojas, S. Mohammed, A.J. Heck, G. Raposo, P. van der Sluijs, J.S. Bonifacino, J. Cell Biol. 183 (2008) 513–526.
[27] M.N. Seaman, M.E. Harbour, D. Tattersall, E. Read, N. Bright, J. Cell Sci. 122 (2009) 2371–2382.
[28] M. Mari, M.V. Bujny, D. Zeuschner, W.J. Geerts, J. Griffith, C.M. Petersen, P.J. Cullen, J. Klumperman, H.J. Geuze, Traffic 9 (2008) 380–393.
[29] J.R. van Weering, P. Verkade, P.J. Cullen, Traffic 13 (2012) 94–107.
[30] T.T. Liu, T.S. Gomez, B.K. Sackey, D.D. Billadeau, C.G. Burd, Mol. Biol. Cell 23 (2012) 2505–2515.
[31] M. Harterink, F. Port, M.J. Lorenowicz, I.J. McGough, M. Silhankova, M.C. Betist, J.R. van Weering, R.G. van Heesbeen, T.C. Middelkoop, K. Basler, et al., Nat. Cell Biol. 13 (2011) 914–923.
[32] J.A. Lewis, J.T. Fleming, Methods Cell Biol. 48 (1995) 3–29.
[33] Q. Ch'ng, L. Williams, Y.S. Lie, M. Sym, J. Whangbo, C. Kenyon, Genetics 164 (2003) 1355–1367.
[34] M. Silhankova, F. Port, M. Harterink, K. Basler, H.C. Korswagen, EMBO J. 29 (2010) 4094–4105.
[35] W. Li, W. Zou, D. Zhao, J. Yan, Z. Zhu, J. Lu, X. Wang, Development 136 (2009) 2445–2455.
[36] J.M. Kinchen, K.S. Ravichandran, Nature 464 (2010) 778–782.
[37] C. Nieto, J. Almendinger, S. Gysi, E. Gomez-Orte, A. Kaech, M.O. Hengartner, R. Schnabel, S. Moreno, J. Cabello, J. Cell Sci. 123 (2010) 2001–2007.
[38] R.S. Kamath, A.G. Fraser, Y. Dong, G. Poulin, R. Durbin, M. Gotta, A. Kanapin, N. Le Bot, S. Moreno, M. Sohrmann, et al., Nature 421 (2003) 231–237.
[39] J.F. Rual, J. Ceron, J. Koreth, T. Hao, A.S. Nicot, T. Hirozane-Kishikawa, J. Vandenhaute, S.H. Orkin, D.E. Hill, S. van den Heuvel, et al., Genome Res. 14 (2004) 2162–2168.
[40] C. Mello, A. Fire, Methods Cell Biol. 48 (1995) 451–482.
[41] A. Raj, P. van den Bogaard, S.A. Rifkin, A. van Oudenaarden, S. Tyagi, Nat. Methods 5 (2008) 877–879.
[42] S.J. Salser, C. Kenyon, Nature 355 (1992) 255–258.
[43] H. Stenmark, Nat. Rev. Mol. Cell Biol. 10 (2009) 513–525.
[44] L. Chotard, A.K. Mishra, M.A. Sylvain, S. Tuck, D.G. Lambright, C.E. Rocheleau, Mol. Biol. Cell 21 (2010) 2285–2296.
[45] H.J. Balderhaar, C. Ungermann, J. Cell Sci. 126 (2013) 1307–1316.
[46] D. Poteryaev, S. Datta, K. Ackema, M. Zerial, A. Spang, Cell 141 (2010) 497–508.
[47] M. Nordmann, M. Cabrera, A. Perz, C. Brocker, C. Ostrowicz, S. Engelbrecht-Vandre, C. Ungermann, Curr. Biol. 20 (2010) 1654–1659.
[48] T.E. Rusten, T. Vaccari, H. Stenmark, Nat. Cell Biol. 14 (2012) 38–45.
[49] W.M. Henne, N.J. Buchkovich, S.D. Emr, Dev. Cell 21 (2011) 77–91.
[50] J.H. Hurley, P.I. Hanson, Nat. Rev. Mol. Cell Biol. 11 (2010) 556–566.
[51] B.M. Collins, S.J. Norwood, M.C. Kerr, D. Mahony, M.N. Seaman, R.D. Teasdale, D.J. Owen, Traffic 9 (2008) 366–379.
[52] A. Hierro, A.L. Rojas, R. Rojas, N. Murthy, G. Effantin, A.V. Kajava, A.C. Steven, J.S. Bonifacino, J.H. Hurley, Nature 449 (2007) 1063–1067.
[53] H. Shi, R. Rojas, J.S. Bonifacino, J.H. Hurley, Nat. Struct. Mol. Biol. 13 (2006) 540–548.
[54] B.M. Collins, C.F. Skinner, P.J. Watson, M.N. Seaman, D.J. Owen, Nat. Struct. Mol. Biol. 12 (2005) 594–602.
[55] S.F. Nothwehr, P. Bruinsma, L.A. Strawn, Mol. Biol. Cell 10 (1999) 875–890.
[56] R. Rojas, S. Kametaka, C.R. Haft, J.S. Bonifacino, Mol. Cell. Biol. 27 (2007) 1112–1124.
[57] J.V. Reddy, M.N. Seaman, Mol. Biol. Cell 12 (2001) 3242–3256.
[58] A.L. Ang, H. Folsch, U.M. Koivisto, M. Pypaert, I. Mellman, J. Cell Biol. 163 (2003) 339–350.
[59] C.M. Hales, R. Griner, K.C. Hobdy-Henderson, M.C. Dorn, D. Hardy, R. Kumar, J. Navarre, E.K. Chan, L.A. Lapierre, J.R. Goldenring, J. Biol. Chem. 276 (2001) 39067–39075.
[60] L. Henry, D.R. Sheff, Mol. Biol. Cell 19 (2008) 2059–2068.
[61] A. Linford, S. Yoshimura, R. Nunes Bastos, L. Langemeyer, A. Gerondopoulos, D.J. Rigden, F.A. Barr, Dev. Cell 22 (2012) 952–966.
[62] M. Sato, K. Sato, W. Liou, S. Pant, A. Harada, B.D. Grant, EMBO J. 27 (2008) 1183–1196.
[63] C. Hsu, Y. Morohashi, S. Yoshimura, N. Manrique-Hoyos, S. Jung, M.A. Lauterbach, M. Bakhti, M. Gronborg, W. Mobius, J. Rhee, et al., J. Cell Biol. 189 (2010) 223–232.
[64] J.C. Gross, V. Chaudhary, K. Bartscherer, M. Boutros, Nat. Cell Biol. 14 (2012) 1036–1045.
[65] K. Beckett, S. Monier, L. Palmer, C. Alexandre, H. Green, E. Bonneil, G. Raposo, P. Thibault, R. Le Borgne, J.P. Vincent, Traffic 14 (2013) 82–96.
[66] P.M. Mangahas, X. Yu, K.G. Miller, Z. Zhou, J. Cell Biol. 180 (2008) 357–373.
[67] S. Seto, K. Tsujimura, Y. Koide, Traffic 12 (2011) 407–420.
[68] J.D. Swarbrick, D.J. Shaw, S. Chhabra, R. Ghai, E. Valkov, S.J. Norwood, M.N. Seaman, B.M. Collins, PLoS One 6 (2011) e20420.
[69] V. Pons, P.P. Luyet, E. Morel, L. Abrami, F.G. van der Goot, R.G. Parton, J. Gruenberg, PLoS Biol. 6 (2008) e214.
[70] Y. Xu, H. Hortsman, L. Seet, S.H. Wong, W. Hong, Nat. Cell Biol. 3 (2001) 658–666.
[71] J.W. Yu, M.A. Lemmon, J. Biol. Chem. 276 (2001) 44179–44184.
[72] C. Frokjaer-Jensen, M.W. Davis, C.E. Hopkins, B.J. Newman, J.M. Thummel, S.P. Olesen, M. Grunnet, E.M. Jorgensen, Nat. Genet. 40 (2008) 1375–1383.